nature climate change

LETTERS

PUBLISHED ONLINE: XX MONTH XXXX | DOI: 10.1038/NCLIMATE1229

Model-based evidence of deep-ocean heat uptake during surface-temperature hiatus periods

Gerald A. Meehl[1]*, Julie M. Arblaster[1,2], John T. Fasullo[1], Aixue Hu[1] and Kevin E. Trenberth[1]

There have been decades, such as 2000–2009, when the observed globally averaged surface-temperature time series shows little positive or even slightly negative trend[1] (a hiatus period). However, the observed energy imbalance at the top-of-atmosphere for this recent decade indicates that a net energy flux into the climate system of about 1 W m^{-2} (refs 2,3) should be producing warming somewhere in the system[4,5]. Here we analyse twenty-first-century climate-model simulations that maintain a consistent radiative imbalance at the top-of-atmosphere of about 1 W m^{-2} as observed for the past decade. Eight decades with a slightly negative global mean surface-temperature trend show that the ocean above 300 m takes up significantly less heat whereas the ocean below 300 m takes up significantly more compared with non-hiatus decades. The model provides a plausible depiction of processes in the climate system causing the hiatus periods, and indicates that a hiatus period is a relatively common climate phenomenon and may be linked to La Niña-like conditions.

Observational datasets derived from the Argo float data and other sources indicate that the ocean heat content above about 700 m did not increase appreciably during the 2000s, a time when the rise in surface temperatures also stalled[6,7]. Hiatus periods with little or no surface warming trend have occurred before in observations, and are seen as well in climate-model simulations[1,8]. So where does the excess heat in the climate system go if not to increase surface temperatures or appreciably increase upper-ocean heat content? There are suggestions that recent increases in stratospheric water vapour[9], stratospheric aerosols[10], tropospheric aerosols[11] or the record solar minimum[11] could have contributed to the most recent hiatus by decreasing the net top-of-atmosphere (TOA) energy imbalance. However, the observational analyses[5] inherently include these effects, and the model analysed here produces close to the observed net energy imbalance during hiatus periods, whereas some modelling studies do not[12]. Alternatively, significant heat could be sequestered in the deep ocean below 700 m on decadal timescales[12–15]. Here we examine simulations from a global coupled climate model to first show that the net TOA energy imbalance in this model is close to what has been observed over the past decade or so. Then we analyse where the heat could be going in the observed system during hiatus periods, and point to the processes that could be responsible.

Five ensemble members from a future-climate-model simulation[16,17] (see Methods) are examined to track the energy flow during the simulation where the net energy flux at the TOA from increasing greenhouse gases is about 1 W m^{-2}, indicating a net energy surplus being directed into the climate system, mainly from decreases in outgoing long-wave radiation[18]. If there are time periods when globally averaged surface temperatures are not increasing, this excess energy must go elsewhere, either to heat the atmosphere and land, to melt ice or snow, or to be deposited in the subsurface ocean and manifested as changes in ocean temperatures and thus heat content. Changes to the cryosphere and land subsurface play a much smaller role than the atmosphere and oceans in energy flows[5], and they are not further considered in this paper.

The time series of globally averaged surface temperature from all five climate-model simulations show some decades with little or no positive trend (Fig. 1a), as has occurred in observations (Supplementary Fig. S1 top). Running ten year linear trends of globally averaged surface temperature from the five model ensemble members reveal hiatus periods (Fig. 1a) comparable to observations (Supplementary Fig. S1 middle). Using the first ensemble member as an example, the overall warming averaged over the century is about +0.15 °C per decade. However, the decades centred around 2020, 2054, 2065, 2070, and several decades late in the century show either near zero or slightly negative trends in that ensemble member. We choose two ten year periods in this ensemble member when the globally averaged surface temperature is negative, that is, less than −0.10 °C over the decade (Fig. 1a), and six similar periods that meet the same criterion from the other four ensemble members, to form an eight-member composite of hiatus periods.

The composite average net energy flux at the top of the atmosphere for the eight hiatus periods (left side of Fig. 1b) is +1.00 [0.88, 1.11] W m^{-2} (the positive sign convention indicates net energy flux into the system), where the values in square brackets are error bars defined as (± one standard error ×1.86) to be consistent with a 5% significance level from a one-sided Student t-test (see Methods). This can be compared with the net energy flux averaged over all other 10 year running-average trends (numbering 435) in the five ensemble members of +1.02 [1.00, 1.04] W m^{-2}. The larger sample reduces the error bars compared with the hiatus decades. The error bars overlap, indicating no significant difference between the eight members in the composite and all other ten year periods, which is equivalent to a significance calculation from a Student t-test (see Methods). Thus in all decades in all five ensemble members there is a radiative imbalance of roughly 1 W m^{-2}. This is indicative of the ongoing increase in CO_2 as well as in positive trends of globally averaged surface temperature that occur in most time periods of the twenty-first century in the model (Fig. 1a). So where is the energy gained by the climate system going during ten year time periods when the globally averaged surface-temperature trend is slightly negative?

As noted above, the most likely candidate is the deep ocean, and this is indeed the case for the model (Fig. 1b for global averages, and Supplementary Fig. S2 by basin). For the upper 300 m layer, the composite global average heat-content trend for the eight decades with negative surface-temperature trend is +0.17 [0.07, 0.27] × 10^{23} J per decade, a reduction of 60% compared

[1]National Center for Atmospheric Research, Boulder, Colorado, USA, [2]CAWCR, Bureau of Meteorology, Melbourne, Australia.
*e-mail: meehl@ncar.ucar.edu; meehl@ucar.edu.

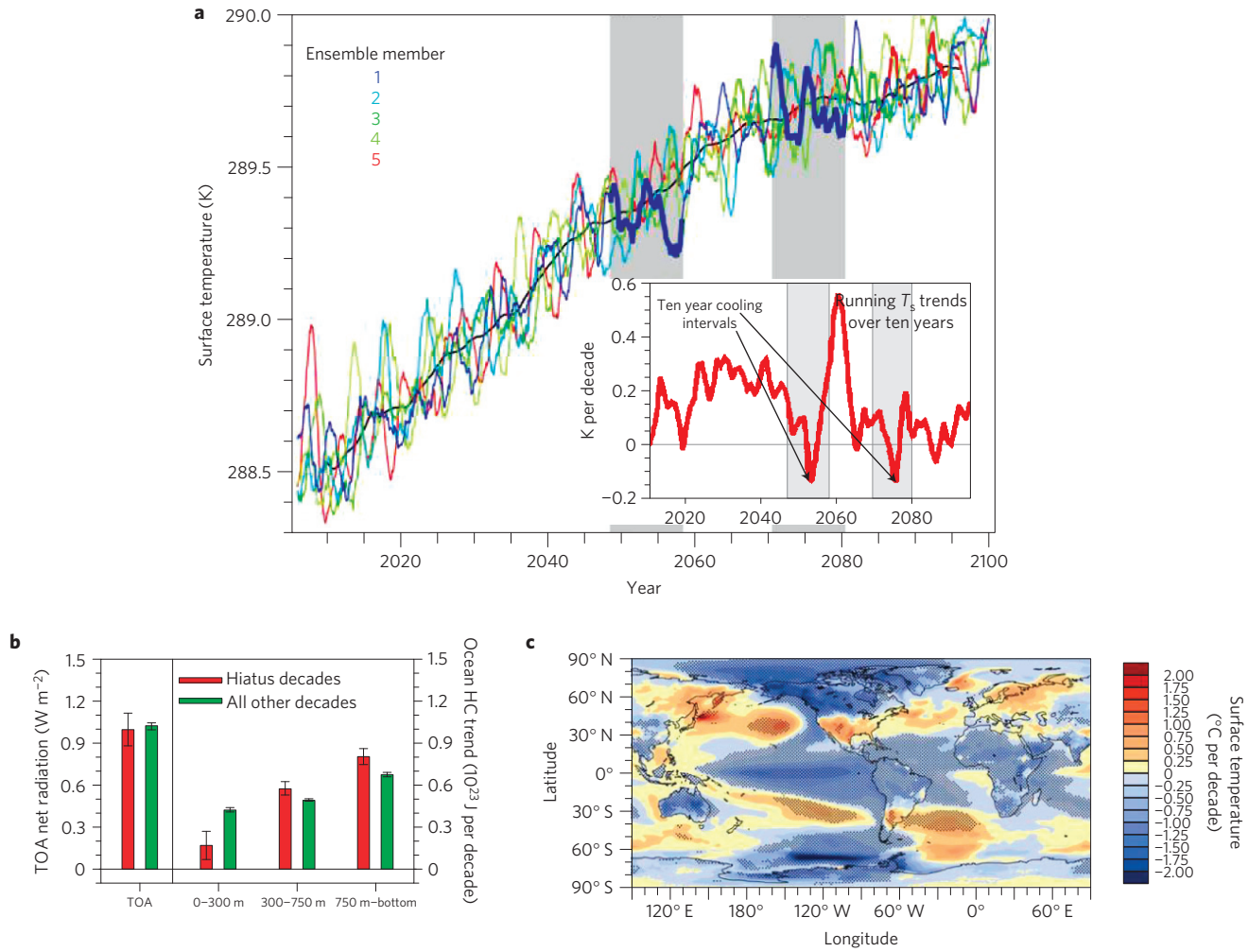

Figure 1 | **a**, Annual mean globally averaged surface temperature for the five climate-model ensemble members (coloured lines) and ensemble mean (black line), highlighting two ten-year negative-temperature-trend periods and ten-year running trends from this ensemble member (inset). **b**, Left: composite global linear trends for hiatus decades (red bars) and all other decades (green bars) for TOA net radiation (positive values denote net energy entering the system). Right: global ocean heat-content (HC) decadal trends (10^{23} J per decade) for the upper ocean (surface to 300 m) and two deeper ocean layers (300–750 m and 750 m–bottom), with error bars defined as ± one standard error ×1.86) to be consistent with a 5% significance level from a one-sided Student *t*-test. **c**, Composite average SST linear trends for hiatus decades; stippling denotes 5% significance.

with the average trend over all decades for the five ensemble members of $+0.42\,[0.41, 0.44] \times 10^{23}$ J per decade. Thus this layer is still gaining heat, but at a much reduced rate during hiatus periods compared with other decades. There is no overlap of the error bars (Fig. 1b), indicating that there is a significant average reduction of the upper-ocean heat-content trend in decades when the surface-temperature trend is slightly negative.

However, in the deeper layers of the global ocean toward the right-hand side of Fig. 1b, the heat-content trends for hiatus time periods are greater than other decades, indicating that most of the excess heat is going into these layers. For the 300–750 m layer the composite global average is 18% larger ($+0.58$ versus $+0.49 \times 10^{23}$ J per decade), and for the layer below 750 m the composite global average is 19% larger ($+0.80 \times 10^{23}$ J per decade compared with $+0.67 \times 10^{23}$ J per decade). The error-bar ranges do not overlap for either layer in Fig. 1b, again indicating that these differences are statistically significant. Thus, during decades of slightly negative surface-temperature trend compared with other decades of positive trend, the trends in global ocean heat content are significantly reduced above 300 m, but significantly increased below 300 m, indicating that more heat is being taken down into the deeper ocean layers of the model.

Examination of ocean heat-content trends by basin (Supplementary Fig. S2) indicates qualitatively similar results to the global ocean, with decreases in heat-content trends above 300 m and increases below 300 m for the hiatus periods compared with all other periods. However, the significance of these changes suggests that different processes are at work in the different basins. In the Atlantic and Southern Oceans, there is a statistically significant reduction of heat content in the upper 300 m (−80% and −70%, respectively). The changes in the 300–750 m layer are not significant, but the trends in the layer below 750 m are statistically significant (+15% and +10%, respectively), indicating that significant excess heat is going deeper in those basins in the hiatus periods. Meanwhile, for the Pacific basin, the increasing trends in ocean heat content for the 300–750 m layer and below 750 m are both statistically significant (+20% and +34%, respectively), similar to the Indian Ocean (+66% and +41%, respectively). Thus, in the Atlantic and Southern Oceans, there is significantly more heat mixed into the deep ocean layer below 750 m, whereas in the Pacific and Indian Oceans there is significantly more heat being deposited in both the mid-ocean layer from 300 to 750 m and the deep ocean layer below 750 m. This redistribution of heat in the ocean is consistent in some ways with what happens on

shorter timescales during El Niño/Southern Oscillation (ENSO; ref. 19). None of the changes in the Arctic basin are significant (not shown), and they are all much smaller than in the other basins in any case.

The eight hiatus periods are characterized by negative sea surface temperature (SST) trends in the tropical Pacific, and positive trends near 30° to 40° N and S latitude in the Pacific and Atlantic that are significant at the 5% level (Fig. 1c). This is similar to the observed pattern of SST trends for a composite of three hiatus periods since the 1970s (Supplementary Fig. S1 bottom), and to the pattern seen in another modelling study[12].

This pattern resembles the La Niña-like negative phase of the Interdecadal Pacific Oscillation[20] that has been attributed to a coupled air–sea tropical-midlatitude mechanism that internally generates decadal timescale variability[21]. The patterns throughout the tropical and subtropical Pacific, Indian and Atlantic Oceans also bear a resemblance to a positive Southern Oscillation (La Niña) pattern[22].

The geographic structure of ocean heat-content changes is denoted by regions where the 20 °C isotherm is deeper during hiatus periods (positive values in Supplementary Fig. S3), indicating that heat may be taken down into the subsurface ocean in these regions. These areas occur near 30° S and 30° N in the Pacific and around 35°–40° N in the Atlantic in regions where there are positive SST trend values (Fig. 1c). Furthermore, stronger trade winds in the Pacific (not shown) are associated with the negative SST trends in the eastern equatorial Pacific, as well as convergence in the western tropical Pacific where warmer water is forced deeper, as indicated by positive values of the anomalies of the 20 °C isotherm there.

The anomalous positive trend values of the depths of the 20 °C isotherm are suggestive of areas where there is convergence of warm surface waters, which then force heat downwards into the deeper ocean. The meridional overturning stream function and associated anomalies are useful in diagnosing such patterns of subsurface ocean warming. The subtropical cells, which are particularly robust in the Pacific[23], are shown by the largest opposite-sign meridional stream-function values above about 700 m between roughly 35° N and S with upward flow near the equator, and convergence and downward flow near 35° N and 35° S (Fig. 2a). The meridional overturning circulation in the Atlantic is illustrated in this global zonal-mean plot as greatest positive values near about 40° N at 1,000 m depth and sinking north of about 45° N. The Ekman divergence in the Southern Ocean near 60° S is shown by maximum positive values centred near 50° S, whereas the Antarctic Bottom Water formation is represented by negative values poleward of about 65° S, and negative values below about 3,000 m that extend into the Northern Hemisphere.

The meridional overturning stream function averaged over the Pacific basin for the layer above about 700 m (Fig. 2b) shows significant positive trend values from about the equator to 40° N, and mostly negative values from near the equator to about 35° S. Such a pattern is indicative of an anomalous strengthening of the subtropical cells in the Pacific during hiatus periods. This produces stronger upward vertical motion near the equator, bringing more cool water to the surface there (negative decadal temperature trends near the equator above about 200 m in Fig. 2c), and greater convergence near the subtropics of each hemisphere that takes warm water downward (for example, positive decadal temperature trends from about 30° to 45° N, and south of 30° S in Fig. 2c). This is consistent with negative SST trends in the equatorial Pacific, and positive SST trends for hiatus decades near 35° to 40° N and S (Fig. 1c). There is mostly small-amplitude warming south of 60° S (Fig. 2c), indicative of a weakening of the Antarctic Bottom Water formation. The bottom-intensified warming that extends north to about 30° S in the Atlantic (Fig. 2e) and to about the equator in the Pacific (Fig. 2c) is also indicative of a weakening of Antarctic

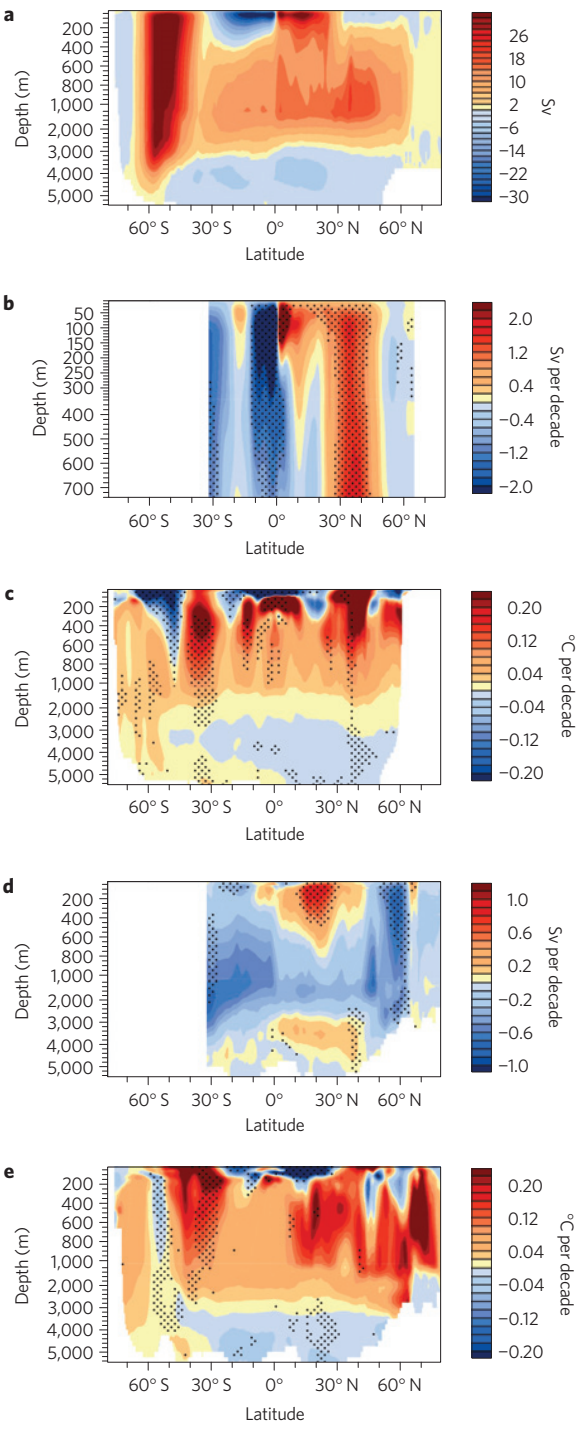

Figure 2 | a, Zonal-mean global long-term-average ocean meridional overturning stream function from the model; positive stream-function contours indicate clockwise flow, negative anticlockwise. **b**, Composite decadal trends of meridional overturning stream function for the upper Pacific Ocean for hiatus periods (note the different vertical scale from **a**; there are no values plotted south of about 35° S owing to the open Pacific basin at those latitudes). **c** The same as **b** except for zonal-mean temperature trends for the Pacific Ocean. **d** The same as **b** except for meridional overturning stream function for the Atlantic Ocean. **e** The same as **b** except for zonal-mean temperature trends for the Atlantic Ocean. Stippling denotes 5% significance.

Bottom Water formation. This warming at depth is noted in the Southern Ocean basin in the model (Supplementary Fig. S2) and in observations[24,25].

In the Atlantic (Fig. 2d), the composite trends in meridional stream function for hiatus decades show positive (negative) trends in the tropical–subtropical North (South) Atlantic in the top few hundred metres, indicating a similar change to that in the Pacific, with a strengthening of the subtropical cell leading to a subsurface warming (Fig. 2e). In the North Atlantic, the composite stream function shows a mostly negative trend, implying a weakening of the deep convection there. As the deep convection weakens, less winter surface cold water moves downward, and indirectly induces a warming effect in the subsurface and deep ocean in the Atlantic[26].

The model provides a plausible depiction of climate-system processes that can cause hiatus periods due to internally generated decadal timescale variability, such as increased subtropical thermocline ventilation in the Pacific and Atlantic (implying increased lower-thermocline heat uptake), and weakened convective mixing in the North Atlantic and Southern Ocean (implying decreased deep-ocean heat loss). Therefore, a hiatus period is a relatively common climate phenomenon even during periods with a sustained radiative imbalance at the TOA of 1 W m^{-2}. Thus, a hiatus period is consistent with our physical picture of how the climate system works, and does not invalidate our basic understanding of greenhouse-gas-induced warming or the models used to simulate such warming.

Tracing changes in global deep-ocean heat content indicated by the model results would require better observed ocean heat-content analyses. In particular, observations of deep-ocean temperatures, which are not generally available now but are planned under Argo, also limit our ability to accurately calculate the sea-level rise contribution due to thermal expansion that depends on ocean heat-content changes[27]. Whether the processes noted here are intrinsically linked through phenomena such as ENSO-like or Interdecadal Pacific Oscillation teleconnections (for example changes in Antarctic Bottom Water formation have been linked to ENSO; ref. 28), or whether it is a coincidence that the oceans change together to play a role in creating the hiatus periods, warrants further exploration.

Methods

The climate model analysed here is the Community Climate System Model version 4 (CCSM4), a global coupled climate model with an approximate 1° horizontal resolution, and 26 levels in the atmosphere, coupled to a 1° (down to 1/4° in the equatorial tropics), 60-level ocean, and state-of-the-art sea-ice and land-surface schemes[16]. Five ensemble members from a future-climate simulation of CCSM4 run under the RCP4.5 scenario[17] are analysed. Although the CO_2 concentrations in the RCP4.5 scenario are beginning to level out near the end of the twenty-first century[17,29], the globally averaged surface temperatures are still increasing (Fig. 1a), partly owing to the increasing CO_2 concentrations, and partly owing to further warming from climate change commitment[30]. We choose RCP4.5 because it is the scenario that has CO_2 increasing at a moderate enough rate that internally generated decadal timescale variability can occasionally offset the forced warming and produce 10 year periods when the surface-temperature trend is slightly negative. Greater increases in CO_2 concentration for the higher-forcing scenario RCP8.5 in the model, for example, do not produce such periods. We examine a future-climate scenario rather than twentieth-century simulations because the latter have combinations of natural and anthropogenic forcings that can produce externally forced periods of little energy imbalance and decreased global warming in certain time periods during the first part of the century[17]. For the time periods from the 1970s up to the present when most of the warming has been anthropogenic in the model[17] there are only four decades to sample. Thus in the future-climate simulations there are many more possible hiatus decades during which the anthropogenic forcing is dominant and ongoing.

Non-overlapping error bars, defined as (±1.86× standard error), are used as a graphical illustration (in Fig. 1b and Supplementary Fig. S1) of statistical significance at the 5% level. In addition to the formal t-test based on the difference between two means, we can show that non-overlapping error bars defined as above imply rejection of the null hypothesis in the one-sided formal t-test. Define X_2 and X_1 as the two mean quantities computed from the two sets of $n = 5$ ensemble members.

Define standard error, $S_1 \equiv \sqrt{S_1^2} = \sqrt{\frac{\sum (X_{1i} - X_1)^2}{n-1}}$ where i runs from 1 to n, and similarly define S_2.

Consider the case when $X_2 > X_1$, consistent with our expectations of a warmer ocean, and thus the use of the one-sided t-test. The non-overlapping error bar criterion says that X_2 and X_1 are significantly different because

$$X_2 - 1.86S_2 > X_1 + 1.86S_1$$

This can be written as

$$X_2 - X_1 > 1.86(S_1 + S_2) \quad (1)$$

By the definition of S_1 and S_2, because

$$S_1 + S_2 \geq \sqrt{S_1^2 + S_2^2}$$

we can say that (1) implies

$$X_2 - X_1 \geq 1.86\sqrt{S_1^2 + S_2^2}$$

which implies rejection of the null hypothesis in a one-sided t-test at the 5% level, because the 95% quantile of a Student t-test with eight degrees of freedom is 1.86.

The statistical significance of the surface-temperature trends (Fig. 1c) is computed from a two-sided Student t-test (used here because we have no expectation of the sign of the SST trend change) of the hiatus trends compared with 435 possible decadal trends across the two ensemble members, with an equivalent sample size, taking into account autocorrelation, of 45 degrees of freedom; similar values are returned when both including and excluding the hiatus trend periods in the larger sample. This methodology is applied to all t-test calculations in this paper.

To calculate the ocean meridional overturning stream function for the Pacific basin north of about 30° S, we subtract the Indonesian Throughflow (12.6 Sv in CCSM4) from the Pacific basin calculation and add this value to the Indian basin.

Received 16 June 2011; accepted 30 August 2011; published online XX Month XXXX

References

1. Easterling, D. R. & Wehner, M. F. Is the climate warming or cooling? *Geophys. Res. Lett.* **36,** L08706 (2009).
2. Hansen, J. *et al.* Earth's energy imbalance: Confirmation and implications. *Science* **308,** 1431–1435 (2005).
3. Trenberth, K. E., Fasullo, J. T. & Kiehl, J. Earth's global energy budget. *Bull. Am. Meteorol. Soc.* **90,** 311–323 (2009).
4. Trenberth, K. E. An imperative for climate change planning: Tracking Earth's global energy. *Curr. Opin. Environ. Sustain.* **1,** 19–27 (2009).
5. Trenberth, K. E. & Fasullo, J. T. Tracking Earth's energy. *Science* **328,** 316–317 (2010).
6. Levitus, S. *et al.* Global ocean heat content 1955–2008 in light of recently revealed instrumentation problems. *Geophys. Res. Lett.* **36,** L07608 (2009).
7. Lyman, J. M. *et al.* Robust warming of the global upper ocean. *Nature* **465,** 334–337 (2010).
8. Santer, B. D. *et al.* Separating signal and noise in atmospheric temperature changes: The importance of timescale. *J. Geophys. Res.* (2011, in the press).
9. Solomon, S. *et al.* Contributions of stratospheric water vapor to decadal changes in the rate of global warming. *Science* **327,** 1219–1223 (2010).
10. Solomon, S. *et al.* The persistently variable 'background' stratospheric aerosol layer and global climate change. *Science* **333,** 866 (2011).
11. Kaufmann, R. K., Kauppib, H., Mann, M. L. & Stock, J. H. Reconciling anthropogenic climate change with observed temperature 1998–2008. *Proc. Natl Acad. Sci. USA* **108,** 11790–11793 (2011).
12. Katsman, C. A. & van Oldenborgh, G. J. Tracing the upper ocean's 'missing heat'. *Geophys. Res. Lett.* **38,** L14610 (2011).
13. Purkey, S. G. & Johnson, G. C. Warming of global abyssal and deep Southern Ocean waters between the 1990s and 2000s: Contributions to global heat and sea level rise budgets. *J. Clim.* **23,** 6336–6351 (2010).
14. Song, Y. T. & Colberg, R. Deep ocean warming assessed from altimeters, gravity recovery and climate experiment, *in situ* measurements, and a non-Boussinesq ocean general circulation model. *J. Geophys. Res.* **116,** C02020 (2011).
15. Palmer, M. D., McNeall, D. J. & Dunstone, N. J. Importance of the deep ocean for estimating decadal changes in Earth's radiation. *Geophys. Res. Lett.* **38,** L13707 (2011).
16. Gent, P. *et al.* The Community Climate System Model Version 4. *J. Clim.* http://dx.doi.org/10.1175/2011JCLI4083.1 (2011).
17. Meehl, G. A. *et al.* Climate system response to external forcings and climate change projections in CCSM4. *J. Clim.* (2011, in the press).

18. Trenberth, K. E. & Fasullo, J. T. Global warming due to increasing absorbed solar radiation. *Geophys. Res. Lett.* http://dx.doi.org/10.1029/2009GL037527 (2009).
19. Roemmich, D. & Gilson, J. The global ocean imprint of ENSO. *Geophys. Res. Lett.* **38,** L13606 (2011).
20. Power, S., Casey, T., Folland, C., Colman, A. & Mehta, V. Interdecadal modulation of the impact of ENSO on Australia. *Clim. Dyn.* **15,** 319–324 (1999).
21. Meehl, G. A. & Hu, A. Megadroughts in the Indian monsoon region and southwest North America and a mechanism for associated multi-decadal Pacific sea surface temperature anomalies. *J. Clim.* **19,** 1605–1623 (2006).
22. Trenberth, K. E. & Caron, J. M. The Southern Oscillation revisited: Sea level pressures, surface temperatures and precipitation. *J. Clim.* **13,** 4358–4365 (2000).
23. McPhaden, M. J. & Zhang, D. Slowdown of the meridional overturning circulation in the upper Pacific Ocean. *Nature* **415,** 603–608 (2002).
24. Kawano, T. *et al.* Bottom water warming along the pathway of lower circumpolar deep water in the Pacific Ocean. *Geophys. Res. Lett.* **33,** L23613 (2006).
25. Johnson, G. C. & Doney, S. C. Recent western South Atlantic bottom water warming. *Geophys. Res. Lett.* **33,** L14614 (2006).
26. Brady, E. C. & Otto-Bliesner, B. L. The role of meltwater-induced subsurface ocean warming in regulating the Atlantic meridional overturning in glacial climate simulations. *Clim. Dyn.* http://dx.doi.org/10.1007/s00382-010-0925-9 (2011).
27. Church, J. A. *et al.* Revisiting the Earth's sea-level and energy budgets from 1961 to 2008. *Geophys. Res. Lett.* **38** (2011, in the press).
28. McKee, D. C., Yuan, X., Gordon, A. L., Huber, B. A. & Dong, Z. Climate impact on interannual variability of Weddell Sea Bottom Water. *J. Geophys. Res.* **116,** C05020 (2011).
29. Moss, R. *et al.* A new approach to scenario development for the IPCC Fifth Assessment Report. *Nature* **463,** 747–756 (2010).
30. Meehl, G. A. *et al.* How much more global warming and sea level rise? *Science* **307,** 1769–1772 (2005).

Acknowledgements

We thank C. Tebaldi for her contributions to the statistical-significance calculations. Portions of this study were supported by the Office of Science (BER), US Department of Energy, Cooperative Agreement No DE-FC02-97ER62402, by the National Science Foundation and by NASA grant NNX09AH89G. The National Center for Atmospheric Research is sponsored by the National Science Foundation.

Author contributions

G.A.M., J.M.A., J.T.F., A.H. and K.E.T. contributed to model data analysis. G.A.M., J.M.A., J.T.F., A.H. and K.E.T. contributed to writing the paper. All authors discussed the results and commented on the manuscript.

Additional information

The authors declare no competing financial interests. Supplementary information accompanies this paper on www.nature.com/natureclimatechange. Reprints and permissions information is available online at http://www.nature.com/reprints. Correspondence and requests for materials should be addressed to G.A.M.

Page 1

Query 1: Line no. 1
Please note that title has been edited as per journal style. OK?

Query 2: Line no. 29
As per journal style, reference citations should be in numerical order. Therefore references are renumbered from here onwards. OK?

Query 3: Line no. 49
Please check the e-mail address is OK as given.

Query 4: Line no. 49
Please provide post codes for all affiliations.

Page 2

Query 5: Line no. 1
Please provide short titles for Figs 1 and 2. Please check y-axis label for fig. 1a.

Page 4

Query 6: Line no. 112
Any update for refs 8, 17, 27?

Query 7: Line no. 116
Please provide page range for ref. 10.

Query 8: Line no. 132
Please provide volume and page range/article id for refs 16, 18, 26.

Page 5

Query 9: Line no. 29
Please confirm the page range given for ref. 29.